

Active Control of a Laminar Separation Bubble

K. Augustin, U. Rist, S. Wagner
Universität Stuttgart, Institut für Aerodynamik und Gasdynamik
Pfaffenwaldring 21, D-70550 Stuttgart, Germany

Summary

In the present paper an active control mechanism for the control of laminar separation bubbles on airfoils is investigated by means of direct numerical simulation and linear stability theory. Boundary layer instabilities excited by periodic oscillations are utilized to control the size and length of the separation bubble and to make it finally disappear when desired. Unlike traditional vortex generators a sensor-actuator system based on this method will be adaptive to the respective flow conditions and will cause no additional undesired drag.

Introduction

Operated in a low Reynolds number regime the drag characteristics of laminar airfoils at “off-design” conditions can be considerably deteriorated by *laminar separation bubbles (LSB)* due to the inability of the laminar boundary layer to overcome the stronger adverse pressure gradient caused e.g. by a higher angle of attack or an extended trailing edge flap. When the laminar boundary layer separates from the airfoil, laminar-turbulent transition may occur and the turbulent boundary layer may reattach to the airfoil because of the increased momentum transfer towards the wall, thus forming a *laminar separation bubble*. To improve the behavior of the airfoil in such an “off-design” situation active control should set in to avoid the occurrence of these bubbles. We suggest to use controlled excitation of boundary layer perturbations upstream of the bubble. These disturbance waves become amplified by instability mechanisms within the laminar boundary layer and in the separation bubble itself which leads to an upstream shift of the transition and the now turbulent boundary layer does not separate. As a constraint the upstream shifting should be achieved by a minimum of disturbance amplitude A_0 respectively of disturbance energy introduced into the flow, but the necessary amplitude A_0 can only be minimized by choosing the proper wavelength λ_x , frequency β and of course the location and length of the disturbance strip exciting sinusoidal disturbance waves.

An indicator for the effectiveness of this control is the location of the point of transition within the LSB as shown in figure 1 where “S”, “T” and “R” mark separation, transition and reattachment, respectively.

The physical investigation of the laminar separation bubble phenomenon by means of *linear stability theory (LST)* and *direct numerical simulation (DNS)* is used to estimate a control method capable to avoid separation in the “off-design” case without deteriorating the design properties of the airfoil.

*Proceedings of the DRAG-NET Conference, June/2000, Potsdam

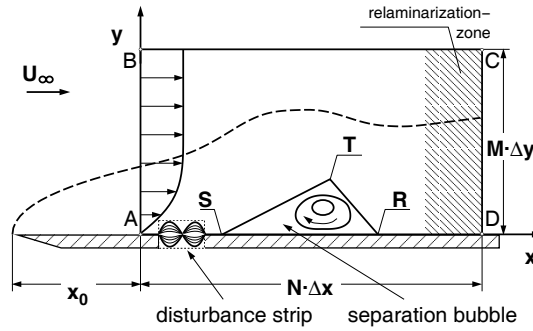
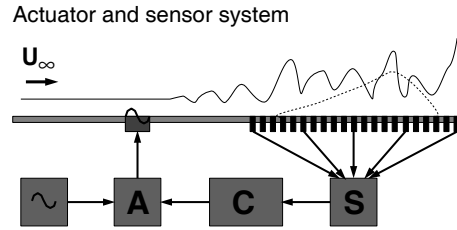


Figure 1: Schematic overview of the integration domain of the DNS with LSB

Based on the considered method an actuator-sensor concept will be designed, where the LSB is detected by sensors and an upstream actuator driven by a controller (figure 2) excites the boundary layer disturbances.


 Figure 2: Sensor (S)-actuator (A) concept with controller (C) and signal generator (\sim)

Numerical method

The implemented 3D DNS method [2] solves the complete *Navier-Stokes* equations for incompressible flow in a vorticity-velocity formulation

$$\frac{\partial \underline{\omega}}{\partial t} - \text{rot}(\underline{v} \times \underline{\omega}) = \frac{1}{Re} \Delta \underline{\omega} \quad (1)$$

with $\underline{v} = (u, v, w)$ and $\underline{\omega} = (\omega_x, \omega_y, \omega_z)$

within a rectangular integration domain (A-B-C-D in figure 1) over a flat plate.

All spatial coordinates are non-dimensionalized by a reference length \tilde{L} and velocities by the freestream velocity \tilde{U}_∞ , where $\tilde{\cdot}$ denotes dimensional variables. This leads, together with the kinematic viscosity $\tilde{\nu}$, to the following definitions for the vorticity vector $\underline{\omega}$ and the frequency β

$$\underline{\omega} = -\text{rot} \underline{v} \quad , \quad \beta = \frac{2\pi \tilde{f} \tilde{\nu}}{\tilde{U}_\infty} \cdot 10^5. \quad (2)$$

Fourth-order accurate finite differences are used on the equidistant numerical grid in stream-wise (x -) and wall-normal (y -) direction whereas a spectral *Fourier* ansatz in spanwise (z -) direction is applied. The explicit time integration is realized by a fourth order, four step *Runge-Kutta* scheme. Once the three vorticity components are obtained, three Poisson equations for the remaining velocities u , v and w have to be computed. Due to the spectral ansatz in spanwise

direction the Poisson equations for the u and v velocity reduce to ordinary differential equations (ODE) and only the v -equation has to be solved iteratively by a line relaxation method accelerated by a multigrid scheme [9].

At the inflow boundary steady *Falkner-Skan* or, at zero pressure gradient, *Blasius* velocity profiles are prescribed. In a relaminarization zone [3] upstream of the outflow boundary the unsteady vorticity components are damped to steady state values to avoid non-physical reflections and as a consequence the unsteady velocity components \underline{v}' vanish exponentially. At the wall the no-slip condition is applied except for a disturbance strip where 2D and 3D perturbations can be introduced into the flow by periodic suction and blowing.

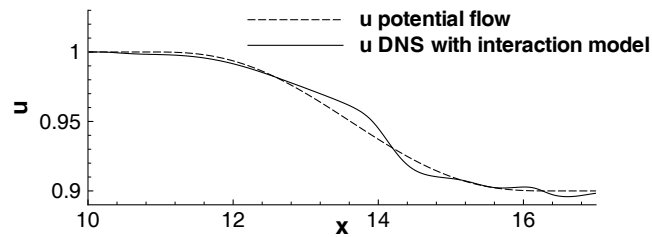


Figure 3: u -velocity distribution at the free-stream boundary

To take into account the strong boundary layer displacement effects of the LSB a viscid-inviscid interaction model is implemented into the multigrid algorithm for the v -velocity component. At run time a velocity distribution which allows for the typical boundary layer displacement effects of a LSB evolves from the initially prescribed potential flow. For a detailed summary of the interaction model and boundary conditions refer to [6]. Figure 3 shows the initial potential distribution of the u -velocity (dashed line) and the resultant distribution considering the effects of the LSB (solid line).

Once the DNS has yielded a reasonable mean flow the development of excited boundary layer perturbations can be studied with less effort by using the *linear stability theory (LST)* [10]. However, the LST provides reasonable results in the linear regime of the disturbance development only, i.e. upstream of the transition ("T") and can not cover variations of the mean flow due to the strong influence of different disturbance amplitudes A_0 on the size of the LSB. Applying the LST the spatial amplification rate α_i of discrete fluctuations specified by their streamwise wavenumber α_r and disturbance frequency β in

$$v(x, y, t) = \hat{V}(y) e^{(\alpha x - \beta t)} \quad (3)$$

with $\alpha = \alpha_r + i \alpha_i$

can be determined by solving the *Orr-Sommerfeld* equation. Values of $\alpha_i < 0$ mean amplification and $\alpha_i > 0$ damping of the disturbance amplitude. The disturbance amplitude A can thereon be obtained by integrating the amplification rate α_i in streamwise x -direction and multiplying these values with an initial disturbance amplitude A_0 .

Disturbance development

To check the accuracy of the DNS and LST results, comparisons to experiments at the laminar wind tunnel at the Universität Stuttgart [5] and at the KTH Stockholm, Sweden [1] have been performed and good agreement of the results has been achieved.

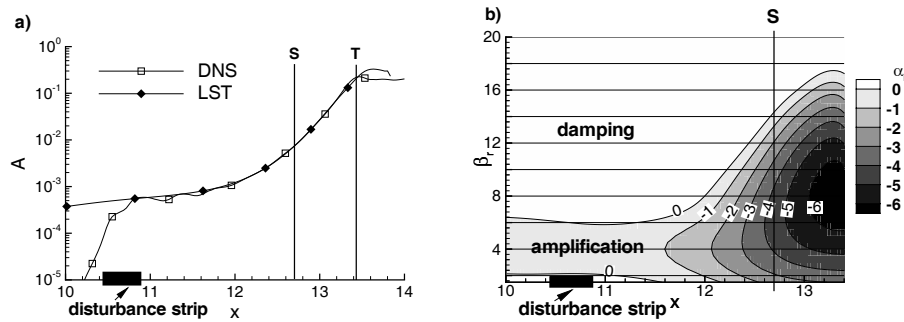


Figure 4: Amplification curves as a result of LST and DNS a) and stability diagram of LST showing amplification rate α_i b)

A comparison of the amplification curves $A = u'_{max}(y)$ for the fundamental disturbance mode (α_r, β) of a typical “midchord-bubble” case at $Re_{\delta_1} = 1722$ at the inflow boundary, considered in greater detail in [8], in figure 4 a) confirms the good agreement between LST and DNS, “S” and “T” again mark separation and transition. Both curves evidently coincide until close to transition which shows that the LST is a proper tool to investigate the disturbance development in flows with LSB. In figure 4 b) the corresponding linear stability diagram $\alpha_i = \alpha_i(x, \beta)$ reveals a narrow band of amplified frequencies β only upstream of the LSB, comparable to a *Blasius* flow, whereas the amplified frequency band broadens further downstream towards the separation line.

For that reason, a suitable disturbance mode for influencing the LSB has to be carefully selected within the amplified frequency band with respect to the streamwise position of the disturbance strip x_0 , its length x_S , wavenumber α_r , wave propagation speed Ω of a travelling wave and initial amplitude A_0 . Langhoff [4] investigated a variety of these parameters in *Blasius* flow where the wall-normal velocities v_0 at the disturbance strip followed the prescription

$$v_0(x, t) = \underbrace{V_0}_{\text{initial amplitude}} \cdot \underbrace{\sin(Bt)}_{\text{amplitude modulation}} \cdot \underbrace{\sin(\alpha_r x - \Omega t)}_{\text{travelling wave}} \quad (4)$$

Depending on the choice of the frequency B for the oscillations at the disturbance strip and of the wave propagation speed Ω different kinds of wall forcing are possible: travelling waves, travelling oscillating waves and standing oscillations. Their ability to excite a *Tollmien-Schlichting* (TS-)wave for a given frequency $\beta = B + \Omega$ is compared in figure 5. It turns out that the boundary layer is most receptive to forcing with travelling waves ($\Omega = \beta$ and $B = 0$). Note that results for two different disturbance frequencies β are shown in figure 5.

For optimal efficiency the position of the disturbance strip for each frequency β should be located in the vicinity of the point where each wave becomes unstable according to LST (so called *branch I* of the neutral stability curve). Only in this case a maximum of integral amplification A can be achieved. At all other positions either the amplitude is damped before the amplified region is reached or the amplified range is too short.

Control of LSB by boundary layer disturbances

An estimation of suitable dimensional disturbance frequencies \tilde{f} for maximum amplification is quoted in table with respect to different free stream velocities \tilde{U}_∞ .

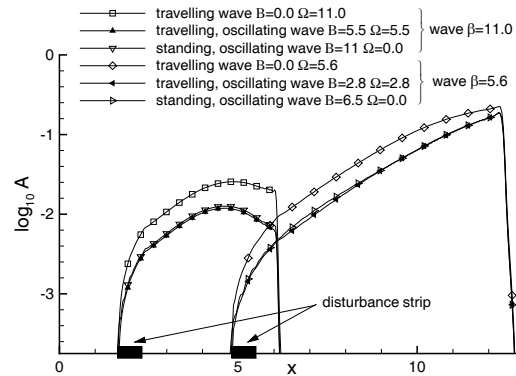


Figure 5: Amplification curves for different waveforms and disturbance frequency

Table 1: Estimation of required dimensional frequencies \tilde{f} with respect to the free stream velocity \tilde{U}_∞

\tilde{U}_∞	$\frac{m}{s}$	20	30	40	50
\tilde{f}	Hz	425	955	1700	2650

The LST allows to estimate the necessary initial disturbance amplitude A_0 to influence the LSB. By integrating the stability diagram (cf. figure 4 b)) in x -direction for every frequency and multiplying with the initial disturbance amplitude A_0 the amplification curves $A = A(x, \beta)$ can be obtained. However, if one specifies a disturbance amplitude A_1 at a position x_1 downstream of the disturbance strip x_0 the necessary initial amplitude A_0 for every frequency β at the disturbance strip to gain A_1 can be determined as shown in figure 6.

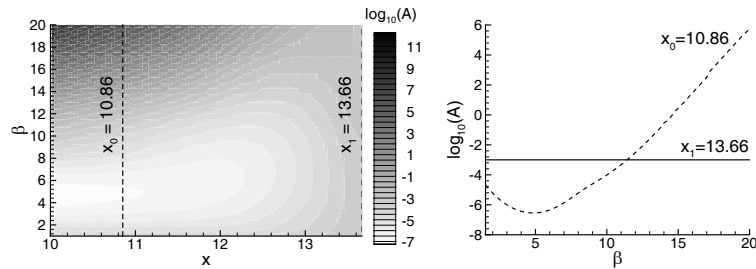


Figure 6: Re-normalized amplitude diagram of LST for amplitude $A_1 = 10^{-3}$ at x_1 ; a) overview and b) cross-section at x_0 and x_1

It is obvious that an appropriate frequency has to be chosen within the amplified frequency band, otherwise the disturbances are damped in such manner that the necessary amplitude A_0 has to be larger than the desired amplitude A_1 at x_1 , which is obviously extremely inefficient. However, if $\beta = 5$ is selected for the disturbance a 1000-fold amplification can be achieved.

Results from simulations of the above mentioned ‘‘midchord bubble’’ with the disturbance amplitude V_0 at a frequency $\beta = 5$ ($B = 5, \Omega = 0$) changing from $V_0 = 10^{-12}$ to 10^{-6} over 120 disturbance cycles T , show that the laminar separation bubble is strongly sensitive with respect to the TS-wave. In figure 7 two results from this simulations at a disturbance level of

$V_0 = 0.89 \cdot 10^{-8}$ and $2.51 \cdot 10^{-8}$ indicate that even a very small change, compared to the free stream velocity, has a lasting effect on the shape of the bubble.

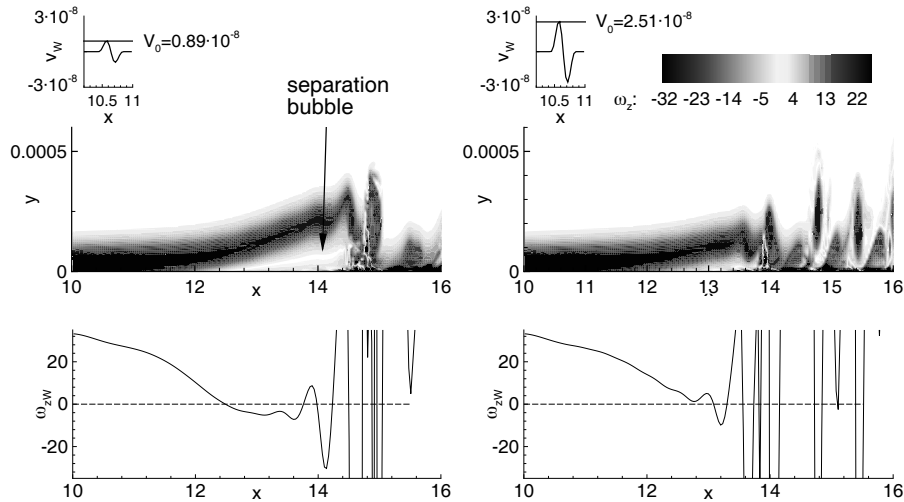


Figure 7: Instantaneous contours of spanwise vorticity ω_z and distribution of skin friction w_{zW} at two different disturbance levels V_0

Beneath the contour figures the corresponding skin friction ω_{zW} curves display the negative shear stress in the area of the LSB as well as the fluctuations of ω_{zW} downstream of the bubble due to vortex shedding in the vicinity of the reattachment line which is also visible from the figures above. The onset of the vortex shedding coincides with the location of transition (“T”) which moves further upstream if the disturbance amplitude is increased. The curve of ω_{zW} on the right hand side shows almost random-like fluctuations at positions (e.g. $x = 14$) where the flow seems to be quite uniform in the left hand side picture. Because of these fluctuations the detection of LSB from instantaneous skin friction data must be avoided and one has to consider time averaged distributions of the skin friction.

Based on the present results a controlling mechanism (cf. figure 2) consisting of an oscillating piezoceramics actuator, which has already been build and tested [7], will be derived. For the present design the oscillation frequency signal for the actuator is provided by a signal generator and only the amplitude V_0 will be controlled. The controller itself will read the signal from the shear stress sensor and determines the size of the LSB by averaging the signal over a certain period of time, e.g. ten disturbance periods. The controller is necessary to avoid excessive disturbance amplitudes, to react on nonlinearities in the control loop, and to enable the mechanism to respond to changing flow conditions where a LSB might not be present.

Conclusion

A method that utilizes the instability mechanisms of a boundary layer flow with laminar separation bubble for amplification of proper disturbances up to an amplitude where an evident change in size of the bubble can be observed has been suggested and investigated by linear stability theory and direct numerical simulation. The simulations will lead to a sensor-actuator system based on wall shear stress sensors and a piezoceramics driven actuator capable of generating the

desired disturbances, which is only activated while a separation bubble is present and otherwise generates no additional drag.

Acknowledgments

The financial support of the Deutsche Forschungsgemeinschaft (DFG) via the Sonderforschungsbereich 409 “Adaptive Strukturen im Flugzeug- und Leichtbau” at the Universität Stuttgart is gratefully acknowledged.

References

- [1] Casper Hildings. Simulation of laminar and transitional separation bubbles. Technical report, Department of Mechanics, Kungliga Tekniska Högskolan (KTH, Royal Institute of Technology), Stockholm, Sweden, December 1997.
- [2] Markus Kloker. Direkte numerische Simulation des laminar-turbulenten Strömungsumschlags in einer stark verzögerten Grenzschicht. Dissertation, Universität Stuttgart, 1993.
- [3] Markus Kloker, Uwe Konzelmann and Hermann F. Fasel. Outflow boundary conditions for spatial Navier-Stokes simulations of transition boundary layers. *AIAA Journal*, 31(4):620–628, April 1993.
- [4] Wolfgang Langhoff. Numerische Untersuchungen zur aktiven Grenzschichtstörungsanregung über schwingende Wandstreifen. Studienarbeit, Institut für Aerodynamik und Gasdynamik, Universität Stuttgart, Januar 1999.
- [5] Ulrich Maucher, Ulrich Rist and Siegfried Wagner. Secondary instabilities in a laminar separation bubble. In Horst Körner and Reinhard Hilbig, editors, *Notes on fluid mechanics (NNFM)*, volume 60, pages 229–236. Vieweg Verlag, 1997.
- [6] Ulrich Maucher, Ulrich Rist and Siegfried Wagner. Refined interaction method for direct numerical simulation of transition in separation bubbles. *AIAA Journal*, 38(8):1385–1393, 2000.
- [7] Jörg Müller. Konzeptstudie für ein aktives Oberflächenfeld zur Verhinderung laminarer Strömungsablösung. Studienarbeit, Bereich Flugzeugentwurf, Fakultät Luft- und Raumfahrttechnik, Universität Stuttgart, September 1999.
- [8] Ulrich Rist. Zur Instabilität und Transition in laminaren Ablöseblasen. Habilitationsschrift, Universität Stuttgart, 1998. Shaker Verlag, 1999.
- [9] Ulrich Rist and Hermann F. Fasel. Direct numerical simulation of controlled transition in a flat-plate boundary layer. *J. Fluid Mech.*, 298:211–248, 1995.
- [10] Hermann Schlichting. *Boundary Layer Theory*, chapter Origin of Turbulence I, pages 459–483. McGraw-Hill, 1979.